

Influence of Initial Ingot Breakdown on the Microstructural and Textural Development of High-Purity Tantalum

J.B. CLARK, R.K. GARRETT, Jr., T.L. JUNGLING, and R.I. ASFAHANI

The influence of initial ingot breakdown on the rolling and recrystallization textures of high-purity tantalum plate was investigated using optical microscopy and X-ray diffraction. The four ingot breakdown processes investigated include two commercial processes and two processes new to tantalum. Correlations among the four ingot breakdown processes, the recrystallized grain size, and the final texture were established. Of the four breakdown processes investigated, the plate from the completely upset-forged ingot had the strongest $\{111\}\langle 110\rangle$ and $\{111\}\langle 112\rangle$ texture components, while the plate from the side-forged ingot recrystallized with a mixed texture. Increased upset forging along the ingot centerline strengthened the $\{111\}\langle uvw\rangle$ orientations and weakened the $\{100\}\langle uvw\rangle$ orientations in the annealed plates. Recrystallization studies were conducted on the rolled plates to develop an optimum texture with both $\{111\}\langle 110\rangle$ and $\{111\}\langle 112\rangle$ texture components in the final recrystallized plate.

I. INTRODUCTION

HISTORICALLY, commercial processing of pure tantalum plate has not required tight control on the microstructural uniformity or crystallographic texture. Electrical properties for lamp filaments and the capacitor industry, corrosion resistance for chemical equipment, and oxidation resistance for high-temperature shielding applications have been the driving requirements.^[1] Therefore, annealed tantalum plate has typically possessed a banded microstructure, exhibiting a mixture of recrystallized and unrecrystallized material, a highly variable grain size, and texture and microhardness gradients, as discussed by the authors in a previous article.^[2] It appears that the banded microstructure is due to insufficient deformation needed to break down the large columnar as-cast microstructure of the electron beam melted (EBM) and the vacuum arc remelted (VAR) tantalum ingots.

Although little recent work has been performed on texture development in tantalum, its body-centered cubic (bcc) structure is the same as steel, so the texture development is expected to be similar. Since the early work of Lankford *et al.*^[3] on steels, it is clear that texture and microstructure have an important influence on the ability of a material to be deep drawn. In low-carbon steels, Emren *et al.*^[4] showed that improved deep-drawing characteristics can be achieved with a fine grain size and a texture consisting of $\{111\}\langle 112\rangle$ and $\{111\}\langle 110\rangle$ orientations. Pokross^[5] showed that it was possible to obtain a fine grain size and $\{111\}\langle uvw\rangle$ texture components in commercially processed tantalum. The goal of this study is to understand the effect of the initial ingot breakdown process on the development of the $\{111\}\langle uvw\rangle$ components in final recrystallized tantalum plate.

A. Processing Procedure

1. Initial ingot breakdown

The starting material came from three 250-mm-long \times 76-mm-diameter VAR tantalum ingots, produced by Cabot Corporation, Boyertown, PA. As-cast microstructures were characterized by analyzing 25-mm-thick sections cut from each of the VAR ingots. Four different ingot breakdown processes were utilized to produce the 32-mm-thick rolling bars. Figure 1 provides a schematic view of each of the four breakdown processes. Two ingots were processed using processing steps that simulate current commercial practices. Process 1 included side forging the ingot into a rolling bar, which is similar to the commercial process employed at Cabot. In process 2, the ingot was upset forged 50 pct and then side forged into a rolling bar. Process 2 is similar to the Fansteel process described by Pokross.^[5]

The third ingot was sectioned into two parts, each being approximately 114-mm long, and the initial ingot breakdown included two processing approaches not previously used for tantalum. In process 3, the half ingot was completely upset forged into a disk 32-mm thick and trimmed into a square plate for ease of subsequent rolling. The other half of the ingot was extruded into a rolling bar, process 4, with the extrusion axis parallel to the original ingot centerline.

For the first three breakdown processes, warm working at less than 773 K was involved. A temperature greater than 773 K had to be used in process 4, the extrusion process. After the initial ingot breakdown, all four of the rolling bars were annealed at 1223 K for 3600 seconds. Samples for metallography and texture studies were sectioned from each of the annealed rolling bars.

2. Rolling and annealing of the plates

For processes 1, 2, and 4, the rolling direction was parallel to the original ingot centerline. For the complete upset process (process 3) the rolling direction was perpendicular to the ingot centerline. The rolling schedule was identical for all of the rolling bars, consisting of unidirectional rolling to 4.6 mm for a total reduction in thickness of 85 pct. After rolling, material from each of the plates was annealed at 1313, 1423, and 1533 K for

J.B. CLARK and R.K. GARRETT, Jr., Materials Engineers, are with the Naval Surface Warfare Center, White Oak, MD 20903-5000. T.L. JUNGLING, formerly with the Naval Surface Warfare Center, is Senior Engineer, Westinghouse Plant Apparatus Division, Monroeville, PA 15146. R.I. ASFAHANI, is Research Project Engineer, U.S.S. Technical Center, Monroeville, PA 15146.

Manuscript submitted March 27, 1991.

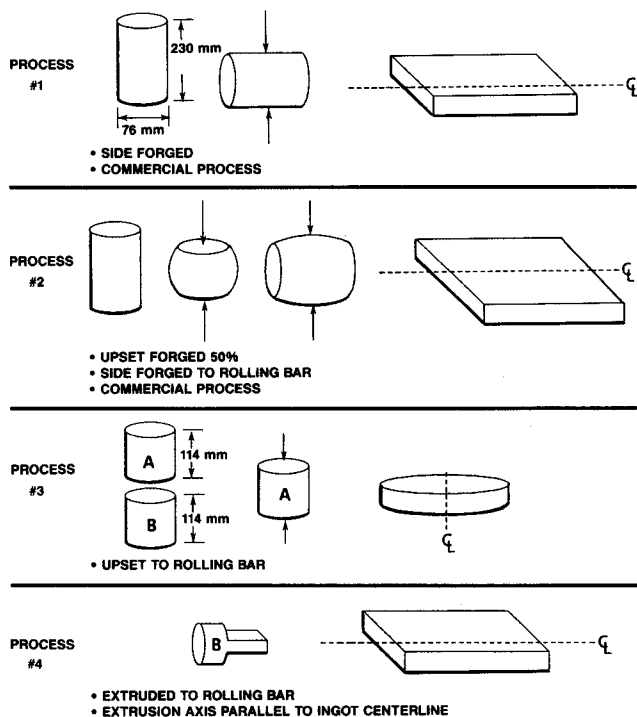


Fig. 1—Schematic view of the four breakdown processes.

3600 seconds in a vacuum furnace. All annealing of the tantalum was conducted in a Brew vacuum furnace to prevent oxidation.

B. Evaluation of Texture and Metallography

Separate texture and metallography specimens were prepared for as-rolled plates from each of the four breakdown processes at each annealing temperature. Measurements of the grain size and the uniformity of microstructure of the recrystallized specimens were accomplished using the Abrams three-circle method (ASTM E112).^[6] Texture specimens were polished and chemically etched prior to being analyzed on a SIEMENS*

*SIEMENS is a trademark of the Siemens Analytical X-Ray Instruments, Inc., Madison, WI.

D-500 diffractometer equipped with a texture goniometer. All of the textures were measured at the mid-thickness of the plates. The Schultz back-reflection technique was used with molybdenum K_{α} radiation to record the (110), (200), (211), and (222) pole figures out to 85 deg from the center. Intensity data were corrected using a random sample of hot isostatically pressed tantalum powder.

Orientation distribution functions (ODFs) were calculated using spherical harmonics analysis. This software used data from the three most intense reflecting planes—(110), (200), and (211)—to calculate the ODFs. The notation in the SIEMENS' software uses Bunge's^[7] notation for the three Euler angles, *i.e.*, PHI, PHI1, and PHI2. For constant PHI1 = 0 deg and PHI1 = 90 deg sections, the {100}<001> orientations are located at the corners of the square, while the {111}<110> orientation is located at PHI2 of 45 deg and PHI of 54.7 deg. During

the rolling of deep-drawing steel, a bcc material, there is an increase in the orientation density for the (001)[110], (112)[110], and (111)[110] orientations, as shown by Emren *et al.*^[4] When the steel is annealed, the orientation density for the (001)[110] and (112)[110] orientations normally decreases, while the orientation density of the (111)[110] orientation normally remains the same. From the ODF sections, two skeletal lines—the alpha fiber and the gamma fiber—were used to describe differences in texture. These skeletal lines have been chosen previously by Emren *et al.*^[4] for the investigation of texture development in deep-drawing low-carbon steels. The alpha fiber shows the orientation density ranging from (001)[110] to (110)[110], while the gamma fiber shows the density for orientations from (111)[011] to (111)[112]. On the ODF, the alpha fiber runs on the constant PHI1 = 0 deg section, at a constant PHI2 = 45 deg, for PHI angles of 0 to 90 deg. The gamma fiber includes the orientation densities located at PHI2 = 45 deg and PHI = 54.7 deg, for PHI1 angles from 0 to 90 deg. Deep-drawing steels tend to develop a strong gamma fiber or strong {111}<uvw>-type components.

II. RESULTS

A. Microstructure of the As-Cast Ingots

The microstructure of the as-cast VAR ingots shows that the grains nucleated near the mold surfaces and grew toward the centerline of the VAR ingot and then parallel to the centerline of the ingot. Figure 2 shows that the columnar grains had a large diameter of approximately 7 mm. It is assumed that the as-cast columnar grains grow in a <100> direction for tantalum, similar to other bcc metals.

B. Intermediate Microstructures of the Rolling Bars

After the vacuum anneal, but prior to rolling, mixed microstructures were observed in the rolling bar. In some cases, the grain size was reduced; but as Figure 3 shows, the recrystallized microstructure depended strongly on the initial ingot breakdown process. For process 1, the rolling bar was essentially unrecrystallized. For the three other processes, the microstructure showed a variety of grain sizes, some fine recrystallized grains and some large grains retained from the original ingot.

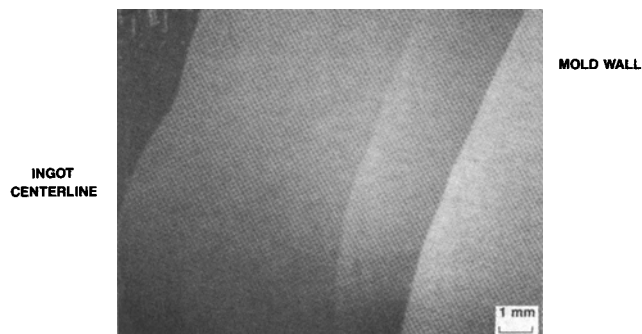
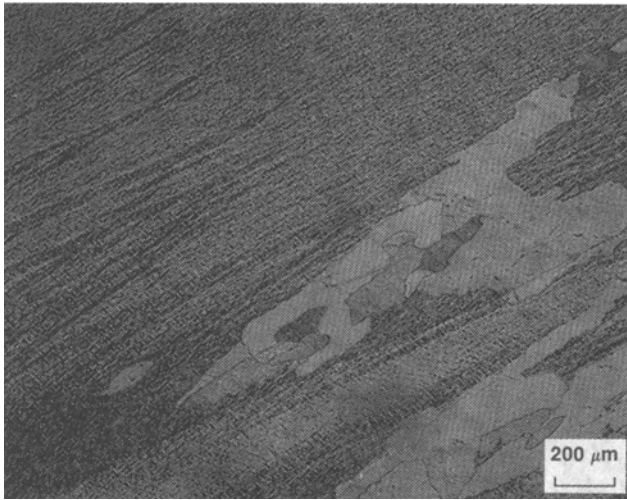
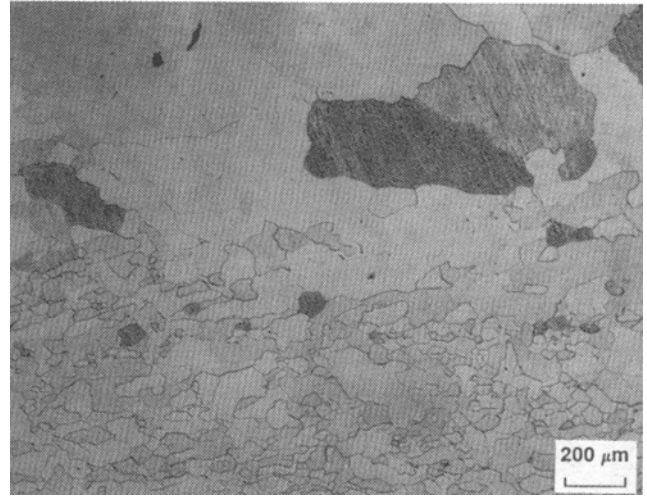


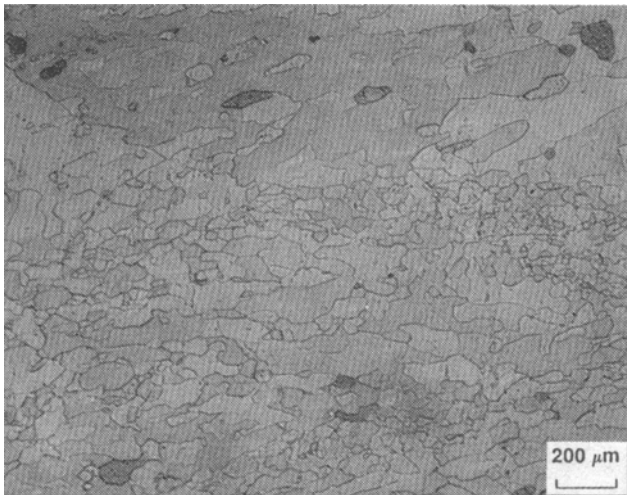
Fig. 2—Microstructure of the as-cast ingots.



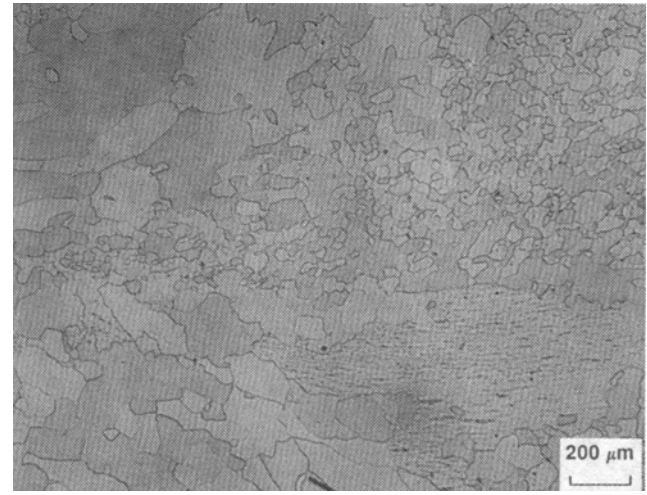
(a) PROCESS #1



(b) PROCESS #2



(c) PROCESS #3



(d) PROCESS #4

Fig. 3—Microstructures of the partially recrystallized rolling bars: (a) process 1, (b) process 2, (c) process 3, and (d) process 4.

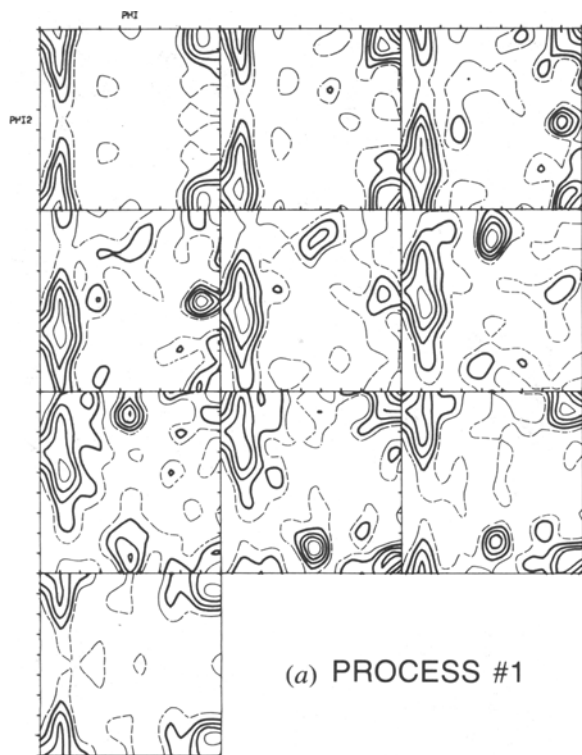
C. Textures of the Annealed Rolling Bars Prior to Rolling

Orientation distribution function results from the annealed rolling bars indicate that processes 1 through 3 had a primary $\{001\}\langle 100\rangle$ texture (the designated plane is normal to the forged surface of the bars and the direction is parallel to the forging direction in the rolling bars). Figure 4 shows the ODF results for the annealed rolling bars. The side-forged bar (process 1) had the strongest (200) central peak intensity of 25 times random on the pole figures, compared to only 4 times random for the 50 pct upset- and side-forged bar (process 2). Side forging did not destroy the original texture of the as-cast columnar grains, so the $\{001\}\langle 100\rangle$ texture remained strong in the rolling bar. The rolling bar from process 4, *i.e.*, the extruded bar, had a mixed texture

with $\{001\}\langle 100\rangle$, $\{113\}\langle 110\rangle$, and $\{011\}\langle 322\rangle$ components.

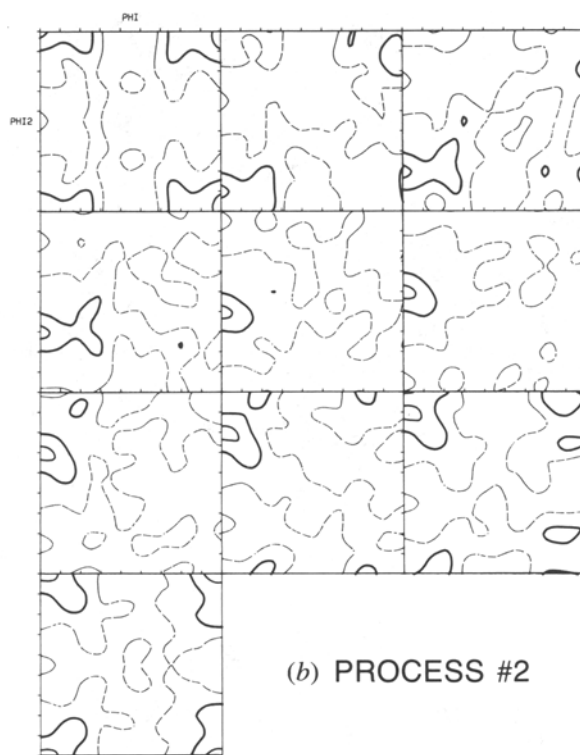
D. Textures of the As-Rolled Plates

Orientation distribution function analysis of the as-rolled plates showed significantly different textures for each of the initial ingot breakdown processes. Normal rolling textures in bcc metals have the following texture components: $\{112\}\langle 110\rangle$, $\{111\}\langle 112\rangle$, $\{001\}\langle 110\rangle$, and $\{111\}\langle 110\rangle$. Process 1 had a mixed texture consisting of $\{100\}\langle 011\rangle$, $\{111\}\langle 011\rangle$, and $\{011\}\langle 211\rangle$ texture components, (Figure 5), but it did not have the $\{112\}\langle 110\rangle$ component found in other bcc metals. The presence of the $\{011\}\langle 211\rangle$ orientation and a lack of the $\{112\}\langle 110\rangle$ orientation implies that the tantalum was



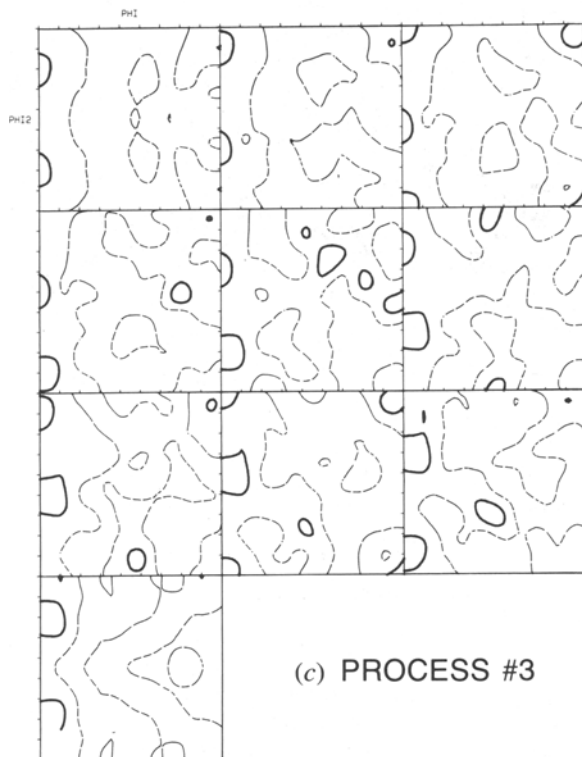
(a) PROCESS #1

SAMPLE: TA0249 CONST. ANGLE: PHI1 = 00, 90, 10
 LMAX = 22; MAX FN HT = 6.09; TSP = 1.23; J INDEX = 2.53
 CONTOURS: 1.0, 2.0, 3.0, 4.0, 5.0, 6.0.



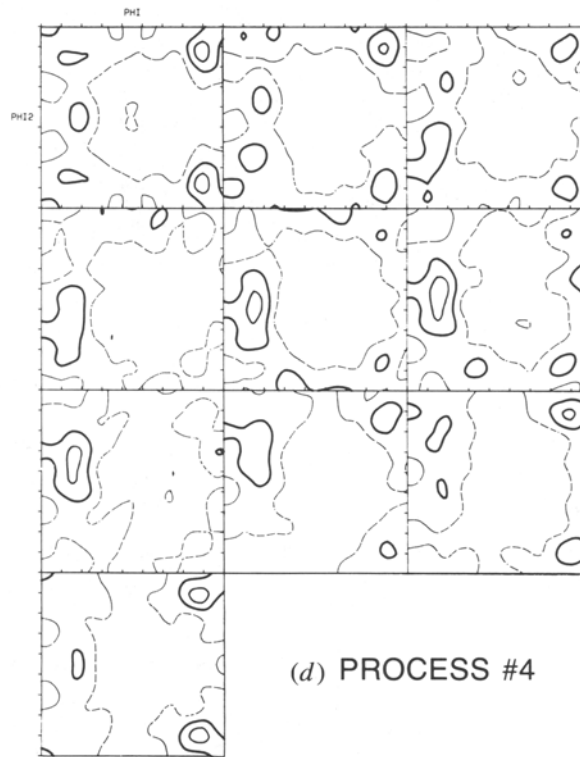
(b) PROCESS #2

SAMPLE: TA0252 CONST. ANGLE: PHI1 = 00, 90, 10
 LMAX = 22; MAX FN HT = 3.25; TSP = 0.53; J INDEX = 1.28
 CONTOURS: 1.0, 2.0, 3.0.



(c) PROCESS #3

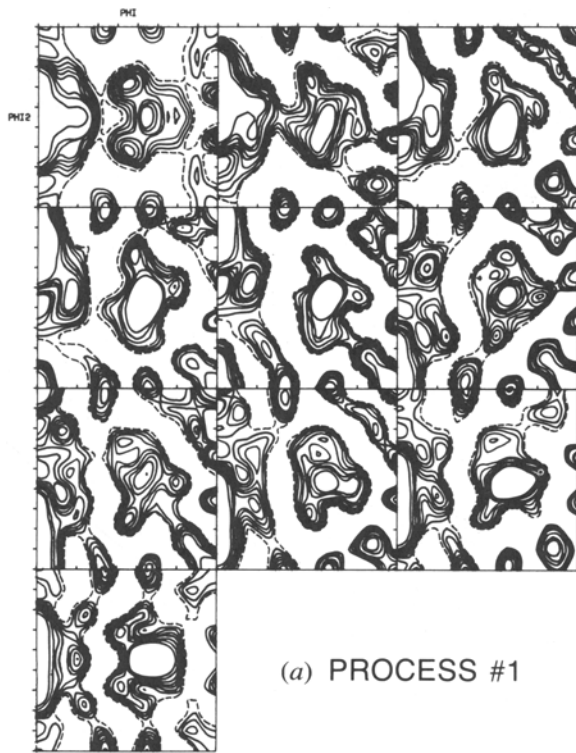
SAMPLE: TA0250 CONST. ANGLE: PHI1 = 00, 90, 10
 LMAX = 22; MAX FN HT = 2.77; TSP = 0.45; J INDEX = 1.20
 CONTOURS: 1.0, 2.0.



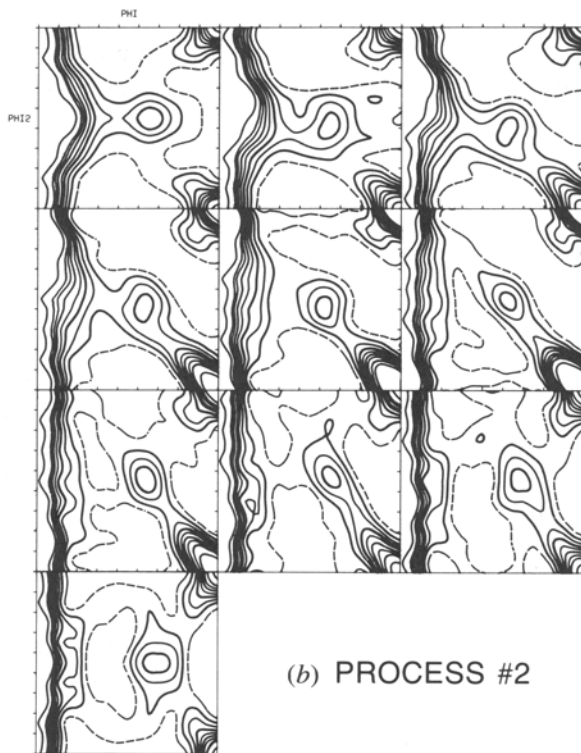
(d) PROCESS #4

SAMPLE: TA0251 CONST. ANGLE: PHI1 = 00, 90, 10
 LMAX = 22; MAX FN HT = 3.57; TSP = 0.62; J INDEX = 1.39
 CONTOURS: 1.0, 2.0, 3.0.

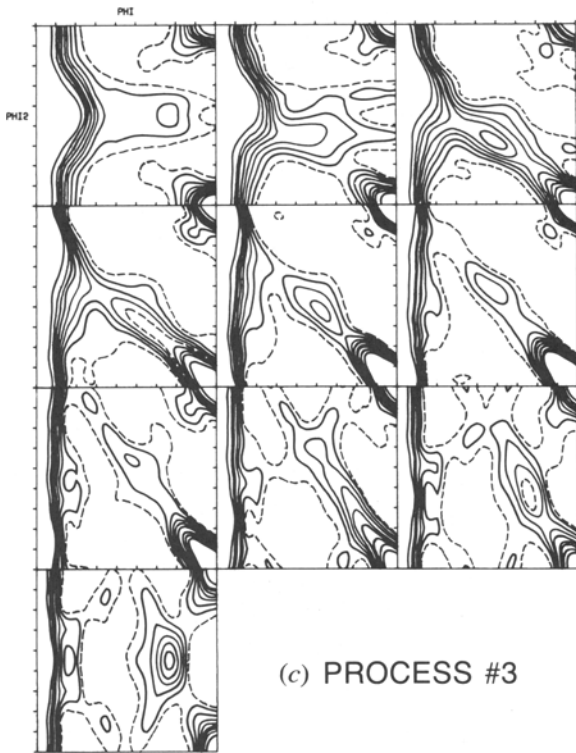
Fig. 4—(a) through (d) ODFs of the annealed rolling bars.



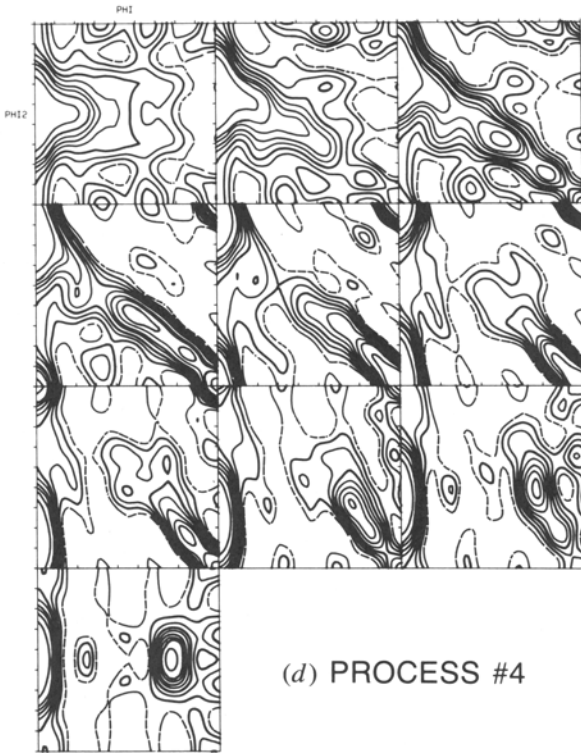
SAMPLE: TA0326 CONST. ANGLE: PHI1 = 00, 90, 10
 LMAX = 22; MAX FN HT = 15.64; TSP = 2.53; J INDEX = 7.38
 CONTOURS: 0.5, 1.0, 1.5, 2.0, 2.5, 3.0, 3.5, 5.0.



SAMPLE: TA0338 CONST. ANGLE: PHI1 = 00, 90, 10
 LMAX = 22; MAX FN HT = 11.98; TSP = 1.27; J INDEX = 2.61
 CONTOURS: 0.5, 1.0, 1.5, 2.0, 2.5, 3.0, 3.5, 5.0.



SAMPLE: TA0330 CONST. ANGLE: PHI1 = 00, 90, 10
 LMAX = 22; MAX FN HT = 16.73; TSP = 1.69; J INDEX = 3.85
 CONTOURS: 0.5, 1.0, 1.5, 2.0, 2.5, 3.0, 3.5, 5.0.



SAMPLE: TA0334 CONST. ANGLE: PHI1 = 00, 90, 10
 LMAX = 22; MAX FN HT = 7.37; TSP = 1.27; J INDEX = 2.61
 CONTOURS: 0.5, 1.0, 1.5, 2.0, 2.5, 3.0, 3.5, 5.0.

Fig. 5—(a) through (d) ODFs of the as-rolled plates.

processed under high body rolling or extreme shear conditions, as discussed by Vandermeer and Bernal.^[8] The three other ingot breakdown processes produced plate with a more typical bcc rolling texture, with components ranging from $\{001\}\langle 011\rangle$ to $\{111\}\langle 011\rangle$. The as-rolled plate from process 3 had the strongest $\{100\}\langle 011\rangle$ component.

E. Microstructures of the Annealed Plates

Table I lists the grain sizes of the annealed plates. All of the material annealed at 1313 K contained unrecrystallized bands. After annealing at 1313 K, plates processed by process 3 appeared to be almost completely recrystallized, with a small unrecrystallized band at midthickness. For processes 1, 2, and 4, the most uniform microstructure recrystallized after annealing at 1423 K. The highest annealing temperature, 1533 K, produced a large grain size for most of the processes and especially for processes 3 and 4. A fine grain size is usually desired for deep drawing applications.

F. Textures of the Annealed Plates

The two commercial processes, 1 and 2, resulted in very similar mixed recrystallization textures with both $\{111\}\langle uvw\rangle$ - and $\{100\}\langle uvw\rangle$ -type components. Process 1 actually exhibits a $\{114\}\langle 110\rangle$ texture, which is near the $\{100\}\langle 110\rangle$ texture. The relative maximum ODF intensities for the various components taken from the ODFs are listed in Table II.

The two new processes resulted in very similar texture results, with strong $\{111\}\langle uvw\rangle$ intensities. Plates from the upset forging process (process 3) had mixed $\{111\}\langle uvw\rangle$ and $\{100\}\langle uvw\rangle$ textures with a strong $\{111\}\langle uvw\rangle$ texture component of 16 times random compared to only 3 times random for the $\{100\}\langle uvw\rangle$ texture. Plate from the extruded bar (process 4) had both $\{111\}\langle 110\rangle$ and $\{111\}\langle 112\rangle$ components with no $\{100\}\langle uvw\rangle$ texture components.

G. Optimization of the $\{111\}\langle uvw\rangle$ Texture Components

Photomicrographs of the plates annealed at the temperature that produced an optimum $\{111\}\langle uvw\rangle$ texture, as indicated by boxes in Table I, are shown in Figure 6. Sections of the ODF ($\text{PHI}1 = 0$ deg) for the four optimum annealing conditions are provided in Figure 7. The optimum temperature was selected as the one that provided the highest intensity for the $\{111\}\langle uvw\rangle$ orientations on the ODF and a low intensity for the $\{100\}\langle uvw\rangle$ orientations. Of the four initial ingot breakdown processes, the plate from the completely upset-forged ingot provided the strongest $\{111\}\langle uvw\rangle$ components in the recrystallized tantalum.

III. DISCUSSION

The results of this study indicate that the initial ingot breakdown process greatly influenced the development

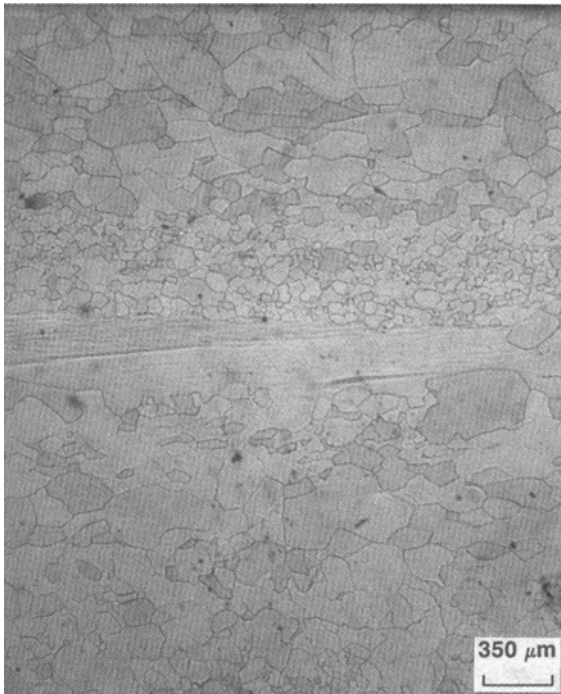
Table I. Grain Size of the Annealed Tantalum (Microns)

Process Number	Process	Annealing Temperature (K)		
		1313	1423	1533
1	side forged	65*	89*	116
2	upset/side	59*	66	82
3	complete upset	38*	78	218
4	extruded	47*	83	244

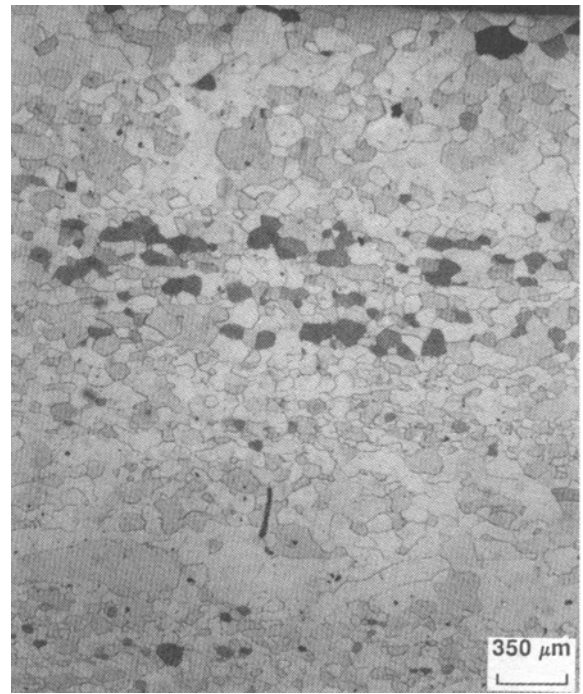
*More than 5 pct unrecrystallized material.
 Optimum $\{111\}\langle uvw\rangle$ fiber texture.

Table II. Summary of Texture Components for the Annealed Plates

Process Number	Process	Annealing Temperature (K)	Maximum Intensity for Each Component			
			$\{111\}$	$\{112\}$	$\{114\}$	$\{100\}$
1	side forged	1313	6	5	—	6
		1423	10	3	6	—
		1533	24	7	4	7
2	upset/side	1313	6	—	3	11
		1423	9	—	—	5
		1533	9	1	—	4
3	complete upset	1313	16	—	—	3
		1423	14	—	4	2
		1533	5	4	3	8
4	extruded	1313	—	3	6	12
		1423	14	—	—	—
		1533	20	—	—	1



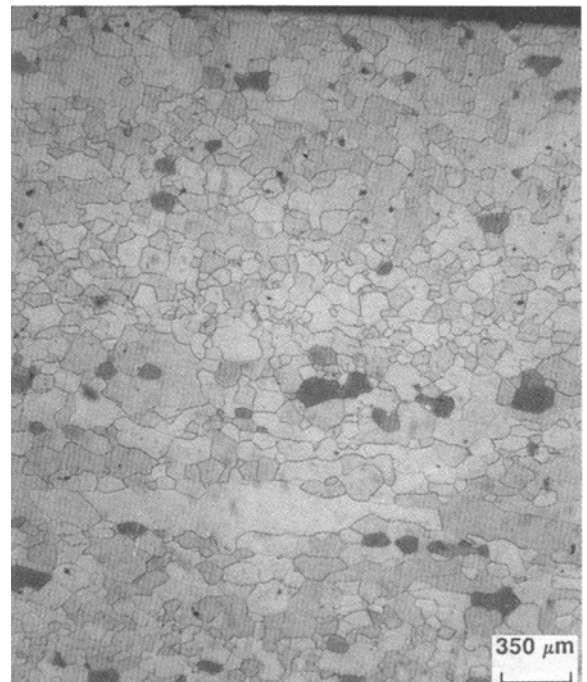
(a) PROCESS #1



(b) PROCESS #2



(c) PROCESS #3

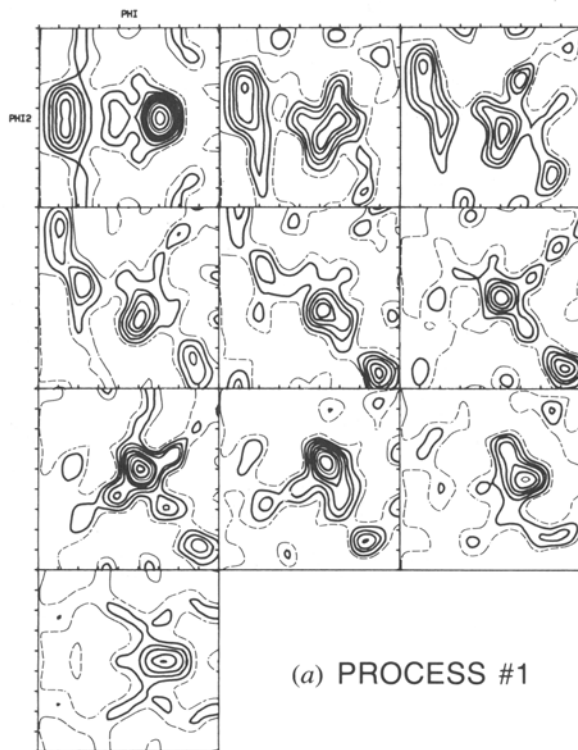


(d) PROCESS #4

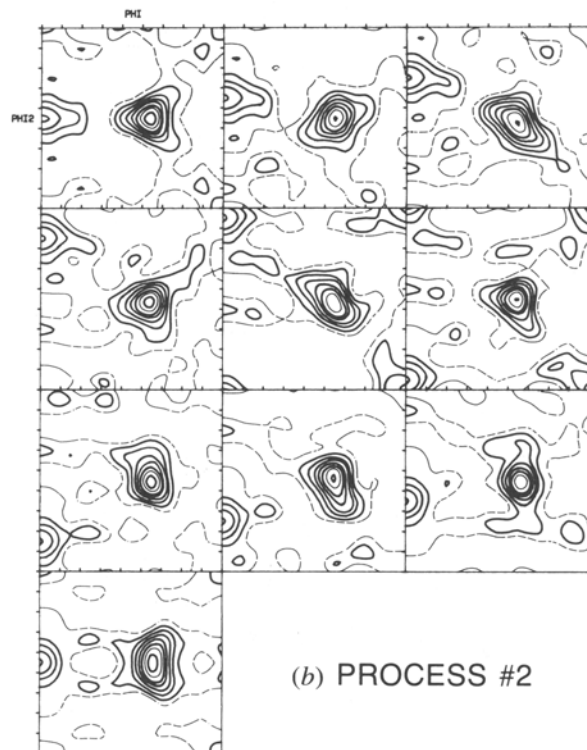
Fig. 6—Microstructures of plates annealed at the optimum annealing temperatures: (a) process 1, (b) process 2, (c) process 3, and (d) process 4.

of crystallographic texture in tantalum and the ability to recrystallize a rolled plate to form strong $\{111\}\langle uvw \rangle$ components in the final recrystallized plate. During the ingot breakdown process, the goal was to introduce work into the ingot to partially recrystallize the as-cast colum-

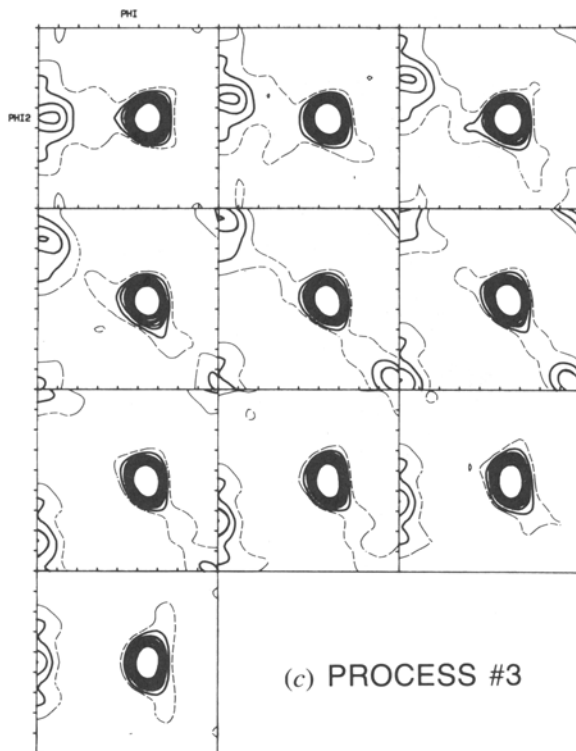
nar grains. These grains probably have a detrimental $\{001\}\langle 100 \rangle$ orientation, as discussed by the authors in a previous article.^[2] In the side-forging process, less cold work was introduced in the axial direction (along the ingot centerline) compared to the other rolling bars. The sum



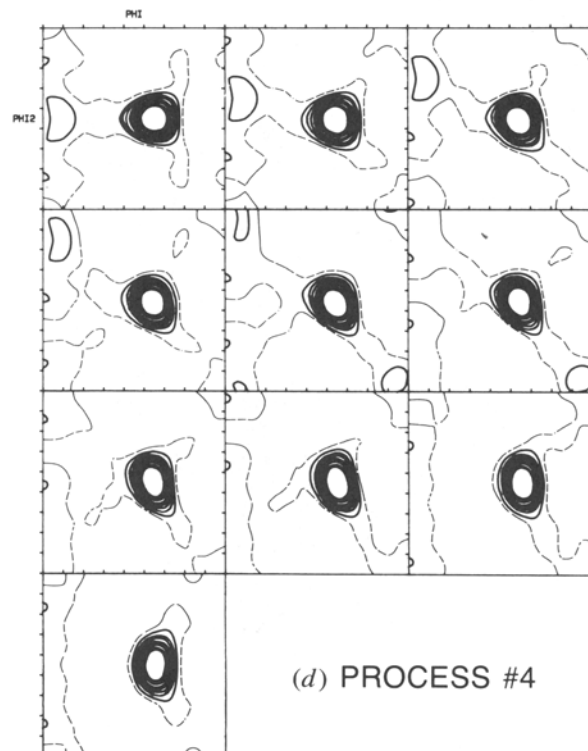
SAMPLE: TA0328 CONST. ANGLE: PHI1 = 00, 90, 10
 LMAX = 22; MAX FN HT = 9.68; TSP = 1.77; J INDEX = 4.13
 CONTOURS: 1.0, 2.0, 3.0, 4.0, 6.0, 7.0, 8.0, 9.0.



SAMPLE: TA0340 CONST. ANGLE: PHI1 = 00, 90, 10
 LMAX = 22; MAX FN HT = 8.79; TSP = 1.53; J INDEX = 3.33
 CONTOURS: 1.0, 2.0, 3.0, 4.0, 6.0, 7.0, 8.0.



SAMPLE: TA0331 CONST. ANGLE: PHI1 = 00, 90, 10
 LMAX = 22; MAX FN HT = 16.44; TSP = 2.28; J INDEX = 6.21
 CONTOURS: 1.0, 2.0, 3.0, 4.0, 6.0, 7.0, 8.0, 9.0.



SAMPLE: TA0336 CONST. ANGLE: PHI1 = 00, 90, 10
 LMAX = 22; MAX FN HT = 13.77; TSP = 2.03; J INDEX = 5.13
 CONTOURS: 1.0, 2.0, 3.0, 4.0, 6.0, 7.0, 8.0, 9.0.

Fig. 7—ODF section for each plate after annealing at the optimum temperature: (a) process 1, (b) process 2, (c) process 3, and (d) process 4 (at constant $\text{PHI1} = 0$ deg).

of the absolute value of the true strains along the ingot centerline was only 0.15, compared to over 1.0 for the three other processes, as listed in Table III. With the decreased level of cold work introduced by the side-forging process in this direction, the rolling bar did not recrystallize at 1223 K, while the rest of the rolling bars were at least partially recrystallized. The rolling bar was still only partially recrystallized by the 1323 K heat treatment. By comparison, the 50 pct upset-forged and side-forged process bar had the highest level of true strain along the ingot centerline, and it was almost completely recrystallized.

The influence of the original ingot breakdown process is also seen in the textures of the final annealed plates. Table I shows that after rolling and further annealing at 1423 K, the plate from the side-forged process was only partially recrystallized, while plates from the other three processes were essentially fully recrystallized. Plates from the upset- and side-forged process had the finest grain size after annealing at both 1423 and 1533 K, while the grain size of the plates from the other three processes were all larger. At a temperature of 1313 K, the plate processed by complete upset forging had the finest grain size. Based on the results from this study, it appears that high strains introduced along the ingot centerline by forging assisted in the recrystallization process of the rolling bar by breaking up the original as-cast columnar grains, thereby creating numerous nucleation sites for subsequent anneals. Rolling strains introduced into the side-forged rolling bar did not add enough work to remove the original columnar grains, and a strong $\{100\}$ -type texture developed in the final recrystallized plate.

The completely upset-forged bar had the strongest $\{111\}\langle uvw \rangle$ components in the final recrystallized plate. Analysis of the cold-rolled texture of this plate showed a strong $\{100\}\langle 011 \rangle$ texture, as shown by the skeletal lines in Figure 8. For tantalum, the presence of the $\{100\}\langle 011 \rangle$ texture indicates a high level of cold work, which seems to aid in the recrystallization of strong $\{111\}\langle uvw \rangle$ components. This is different from the results of deep-drawing steel, where a $\{112\}\langle 011 \rangle$ rolling texture was a prerequisite to the nucleation of the $\{111\}\langle 112 \rangle$ grains.^[9]

The final grain size of rolled and recrystallized steel has been shown by Emren *et al.*^[4] to depend strongly on the starting grain size. If the original grain size was large, then the grain size of the final recrystallized steel tended to be large. For tantalum, the original as-cast grains in the VAR ingots were very large, as seen in Figure 2. The annealing temperature, after the initial ingot breakdown, was chosen as the temperature at which the rolling bars had just started to recrystallize. It appears that the partially recrystallized microstructure provides more

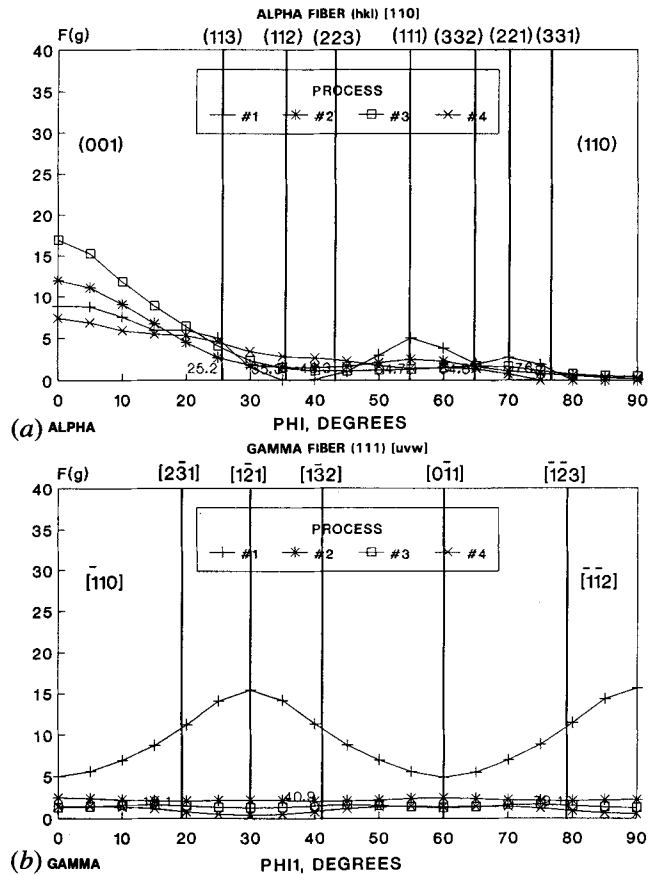


Fig. 8—(a) Alpha and (b) gamma fibers from the as-rolled plates.

nucleation sites for the growth of the desired $\{111\}\langle 112 \rangle$ and $\{111\}\langle 110 \rangle$ oriented grains. After the ingot breakdown, if the rolling bar is not annealed, then the rolled plate recrystallizes with a mixed texture consisting of $\{111\}\langle 110 \rangle$ and $\{100\}\langle 011 \rangle$ orientations in the final plates. Single-crystal studies by Vandermeer and Snyder^[10] have shown that the $\{100\}\langle 110 \rangle$ -oriented grains deform less and do not readily recrystallize but only recover. By comparison, the $\{111\}\langle uvw \rangle$ -oriented grains deform to a greater extent and recrystallize with a finer grain size. In this work, the columnar grains in the VAR ingot apparently had a $\{100\}\langle uvw \rangle$ -type orientation, which made it difficult to introduce deformation into the microstructure, so it was more difficult to recrystallize the rolling bar. For these studies, a lower annealing temperature was selected to partially recrystallize the microstructure, because a higher rolling-bar annealing temperature would have produced a larger grain size in the recrystallized plate.

Table III. True Strains Involved in the Ingot Breakdown Processes

Process Number	Process	Axial Strain	Thickness Strain	Width Strain
1	side forged	0.15	0.875	0.47
2	upset/side	1.508	1.565	0.505
3	complete upset	1.28	0.64	0.64
4	extruded	1.04	0.88	0.41

Rolling parallel to the ingot centerline for processes 1 and 2 did not reduce the $\{100\}\langle uvw \rangle$ texture components. Even after rolling to a reduction of 85 pct followed by annealing, the texture still consisted of mixed $\{111\}\langle uvw \rangle$ - and $\{100\}\langle uvw \rangle$ -type textures, as shown in Figure 9. Side-forged plate, process 1, had the weakest $\{111\}\langle 110 \rangle$ texture. It appears that upset forging along the ingot centerline is necessary to recrystallize a plate with a $\{111\}\langle uvw \rangle$ texture component.

IV. CONCLUSIONS

1. Tantalum plates processed by upset forging, followed by rolling, provided recrystallized plate with strong $\{111\}\langle 112 \rangle$ and $\{111\}\langle 110 \rangle$ texture components and a fine grain size.
2. Plates processed by side forging had a detrimental $\{001\}\langle 100 \rangle$ texture in the rolling bar which could

- not be removed by subsequent plate rolling and annealing.
3. A combination of upset and side forging or extrusion, followed by rolling and annealing, produced plates with mixed $\{111\}\langle uvw \rangle$ and $\{100\}\langle uvw \rangle$ textures.
4. Rolling parallel to the ingot centerline in material that has not been upset forged did not remove the $\{001\}\langle 100 \rangle$ orientation found in the annealed rolling bars. These orientations were apparently carried over from the large columnar grains of the original VAR ingot.
5. It is possible to process tantalum ingots via upset forging or extrusion, followed by rolling and annealing, in order to produce recrystallized plate with strong $\{111\}\langle uvw \rangle$ texture components.

ACKNOWLEDGMENTS

This research was funded by the Office of Naval Technology through Dr. William Messick, the Block Program Manager at the Naval Surface Warfare Center (NAWSWC). The authors would like to express their appreciation to C. Whipps for preparing the many metallography and texture samples and to M. Shephard for running all of the texture samples on the SIEMENS D500 TX system at NAWSWC. They would also like to thank Dr. R.A. Vandermeer of the Naval Research Laboratory for reading and discussing the manuscript. The authors are also appreciative of Cabot Corporation and its technical staff for producing the ingots and for their helpful technical comments.

REFERENCES

1. M. Semchyshev and J.J. Harwood: *Refractory Metals and Alloys*, TMS, Warrendale, PA, 1961, pp. 357-81.
2. J.B. Clark, R.K. Garrett, Jr., T.L. Jungling, R.A. Vandermeer, and C.L. Vold: *Metall. Trans. A*, 1991, vol. 22A, pp. 2039-48.
3. W.T. Lankford, S.C. Synder, and J.A. Bauscher: *Trans. ASME*, 1950, vol. 42, pp. 1197-1232.
4. F. Emren, U. Von Schlippenbach, and K. Lucke: *Acta Metall.*, 1986, vol. 34 (11), pp. 2105-17.
5. C. Pokross: *J. Met.*, 1989, October, pp. 46-49.
6. *Annual Book of ASTM Standards*, E 112-85, ASTM, Philadelphia, PA, 1987, vol. 3.01, pp. 403-36.
7. H.J. Bunge and C. Esling: *Quantitative Texture Analysis*, Informationsgesellschaft, Germany, 1986, pp. 3-72.
8. R.A. Vandermeer and J.B. Bernal: *Texture Cryst. Solids*, 1977, vol. 2, pp. 183-203.
9. U. Von Schlippenbach, F. Emren, and K. Lucke: *Acta Metall.*, 1986, vol. 34 (7), pp. 1289-1301.
10. R.A. Vandermeer and W.B. Snyder, Jr.: *Metall. Trans. A*, 1979, vol. 10A, pp. 1031-44.

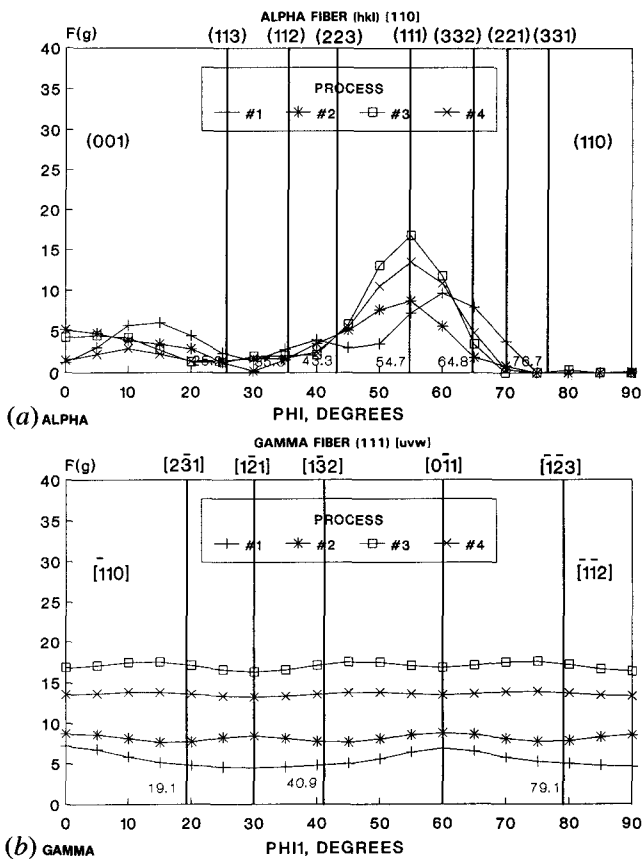


Fig. 9—(a) Alpha and (b) gamma fibers from the anneal optimization study.